Hindawi
Geofluids
Volume 2023, Article ID 4282387, 10 pages
https://doi.org/10.1155/2023/4282387

*Research Article*

# Nanometer-Scale $CO_2$-Shale Oil Minimum Miscibility Pressure Calculations Based on Modified PR-EOS

**Yahui Bu,[1] Qian Sun,[2,3] Shuoran Fu,[3] Lingkong Guo,[3] and Na Zhang [2,3]**

[1]*Exploration and Development Research Institute, Shengli Oilfield Company, SINOPEC, Dongying, Shandong 257061, China*
[2]*College of Petroleum Engineering, Shandong Institute of Petroleum and Chemical Technology, Dongying, Shandong 257061, China*
[3]*College of Energy Resources, Chengdu University of Technology, Chengdu, Sichuan 610059, China*

Correspondence should be addressed to Na Zhang; znpear@163.com

Received 28 December 2022; Revised 24 February 2023; Accepted 17 April 2023; Published 19 May 2023

Academic Editor: Yueliang Liu



CO2 flooding is recognized as an efficient method for enhancing shale oil recovery, while CO2-oil MMP (minimum miscibility pressure) in the micro-nanoscale is a crucial parameter. This paper presents a method for calculating the MMPs of pure hydrocarbons (C4H10, C6H14, C8H18, and C10H22) and CO2 systems in nanopores (3 nm to 10 nm) with temperature ranging from 290.15 K to 373.15 K. Firstly, we modify the Peng-Robinson equation of state (PR-EOS) by considering the influence of confinement effect and capillary pressure in nanopores. Secondly, the flash calculation algorithm is employed to determine whether the oil and gas phases in nanopores have reached an equilibrium state according to the equality of the fugacity of the two phases. Thirdly, we calculate the interfacial tension (IFT) between the two phases using the Macleod-Sugden equation. When the extrapolated IFT is zero, we treat the corresponding pressure as the MMP of the CO2-oil system in nanopores. Simulation results indicate that the calculated MMP using this method has a relative error of about 0.62% compared to the MMP calculated using the multiple mixing cell (MMC) method, indicating high reliability for MMP prediction. Moreover, the measured MMP at the nanoscale is generally smaller than that in the bulk phase due to the influence of the confinement effect. The MMP is positively correlated with the reservoir temperature, the carbon atom number in alkanes, and the nanopore radius.

## 1. Introduction

With the continuous development of the social economy in China, the total demand for energy is also constantly increasing. According to the latest data in 2021, the total oil imports reached 512.98 million tons in China, and the dependence on foreign oil reached 72.05% [1]. Therefore, the issue of energy security cannot be ignored. In addition, many oilfields have entered the production decline stage. And the crude oil recovered with existing technology is of poor quality and has low recovery. To alleviate the crisis of energy shortage and achieve self-sufficiency in crude oil production, it is essential to develop unconventional reservoir resources with richer reserves [2, 3].

The shale oil reserves in China are extremely considerable. And the total crude oil in place is as high as 47.64 billion tons, while the total technically recoverable reserves are 15.97 billion tons. It is dominated by continental shale oil which includes medium-low maturity shale oil and medium-high maturity shale oil [4]. However, the exploitation of shale oil reservoirs is particularly difficult. The reason is that the porosity and permeability of shale oil reservoirs are low, and the brittle minerals and clay minerals in reservoirs are well developed. Besides, the heterogeneity in shale oil reservoirs is strong [5]. The methods to exploit the shale oil reservoirs mainly include the multiple-stage fracturing technology for horizontal wells, the exploitation technology by continuous gas injection, the exploitation technology by cyclic gas injection, the gas injection huff and puff technology, and so on [5]. The $CO_2$ injection huff and puff technology has a better effect on improving shale oil recovery [6]. Exploiting the shale oil reservoirs by injecting $CO_2$ can not only increase the total production of shale oil but also realize the rational use and geological storage of $CO_2$. Meanwhile, it

is also an important technology to achieve carbon capture, utilization, and storage (CCUS). Liu and Rui suggested that applying $CO_2$ flooding in oilfields can be an effective method for reducing $CO_2$ emissions by storing the $CO_2$ in oil reservoirs [7]. The storage-driven $CO_2$ EOR can even realize net-zero or even negative $CO_2$ emissions [8]. The addition of certain cosolvents, such as propanol or dimethyl ether, can enhance the solubility of $CO_2$ in oil, thereby improving the effectiveness of $CO_2$-enhanced oil recovery ($CO_2$-EOR) [9]. It is an innovation to solve the greenhouse effect problems and protect the ecological environment [10–12]. The mechanisms of $CO_2$ injection to enhance oil recovery mainly include the following: (1) reducing the viscosity of crude oil and improving the fluidity of crude oil; (2) making the volume of crude oil expand and part of the shale oil break away from the shackles of the formation to increase the internal kinetic energy; (3) replacing the adsorbed shale oil through equimolecular replaceability and extracting the light hydrocarbon components to reduce the remaining oil saturation; (4) reducing the oil and water interfacial tension (IFT) and the resistance of oil displacement; (5) making $CO_2$ and shale oil realize miscible and reducing the flow resistance of the remaining oil in the millimeter to nanometer pores; and (6) carbonated formation water can be dissolved to eliminate scaling and blockage and improve the formation permeability; (7) $CO_2$ dissolved gas flooding, which can not only supply the formation energy but also promote the flow of shale oil in pores and fractures [13–16]. Among them, the miscibility of $CO_2$ and shale oil has an important impact on the improvement of shale oil recovery. When the formation pressure is greater than the minimum miscibility pressure (MMP) of the oil and $CO_2$, the oil and $CO_2$ miscibility makes the interfacial tension between oil and $CO_2$ turn zero. Therefore, the shale oil in the nanopores can be largely extracted. And the efficient exploitation of shale oil reservoirs is realized.

MMP is a crucial parameter to verify whether $CO_2$ and crude oil are miscible or not. It is significant to obtain the oil-$CO_2$ MMP in the micro-nanoscale [17–20]. The methods for determining the MMP primarily involve experimental methods and theoretical calculation methods [21]. The slim tube experiment is recognized as the most reliable standard test method [22, 23]. It can simulate not only the oil and gas displacement in one-dimensional space but also the complex system of three phases. However, this experimental method also has some disadvantages that cannot be ignored. Firstly, this method is time-consuming and costly [24, 25]. Compared with the slim tube experiment, the vanishing interfacial tension (VIT) technique is simple in operation and less time-consuming. At the same time, the method is more rigorous, and the measured MMP is more accurate [26]. However, it is not suitable for multicontact miscible systems, and it would be affected by subjective factors [27]. The multicontact experiment method has the advantages of high efficiency, high precision, and low cost. Meanwhile, the MMP measured by the multicontact experiment method is generally under the condition of a single condensing drive or vaporizing drive [28]. But the real miscibility of gas flooding is usually achieved by the combination of condensing and vaporizing drives. Therefore, this method cannot accurately measure the MMP [29]. For the rising bubble method, it is low-cost, has a short experimental cycle, and has reliable results [30]. However, this method can only measure the MMP of oil-gas miscibility under the condition of the vaporizing drive. So it is not suitable for the measure of MMP, whose miscible mechanism is condensing drive or condensing-vaporizing drive [31]. The steam density method is low in expenditure and short in the experimental cycle [32]. Nevertheless, it is generally carried out at a low temperature, and the measured MMP in the experiment needs to be converted into the value at the real formation temperature. There may be some errors in the experimental results by using this method [33].

In order to find a faster way to determine MMP, scholars obtain empirical correlations by fitting the relevant experimental data. A large number of empirical correlations have been proposed, such as the Glaso correlations, Johnson-Pollin correlations, and Alston correlations [34–36]. Compared with the experimental method, the empirical correlation method is simple, convenient, and low-cost. However, the empirical correlation is only applicable to the calculation of MMP under specific reservoir conditions. Once the target reservoir conditions change, the calculation results may have large errors. So, this method is not a general theoretical calculation method. Compared with the experimental method, the method of characteristics (MOC) can quickly give the predicted value of MMP, which does not depend on the movement of the oil phase and gas phase. And the two phases can fully contact to be miscible when using MOC [30]. It is also applicable to pure $CO_2$ and crude oil, which helps researchers understand the characteristics of gas flooding. However, this method is only suitable for pure $CO_2$ and crude oil. And the calculation process is complex, and it is difficult to converge to the correct key tie line [37, 38]. In addition, there are some potential problems, which result in the low prediction accuracy of MMP in the negative flash calculation [38]. The one-dimension slim tube compositional simulation method can reflect the oil-gas flow state in porous media by using the numerical simulation method to simulate the slim tube experiment. This method can simulate complex three-phase systems. There may be a deviation in MMP due to the influence of numerical dispersion effects [39]. Although using the high-order method can mitigate the dispersion effect, it cannot completely remove its influence. Furthermore, the instability of the three-phase equilibrium calculation and the fuzzy permeability model also make the predicted MMP inaccurate. The multiple mixing cell (MMC) method is a method that simulates the contact and mixture of oil and gas. Initially, two cells involve the injection gas and the reservoir oil at a fixed temperature and pressure. Then, it obtains new oil and gas components after two-phase miscibility equilibrium, and the new oil and gas components contact and mix separately again with the original gas and oil components. Finally, constantly repeat this process until all the key tie lines are found and converge to the specified tolerance. This method has two common models, one is the AHMADI model and another is the JAUBERT model, as shown in Figures 1 and 2 [40, 41]. The MMC model can predict the MMP of two-phase systems

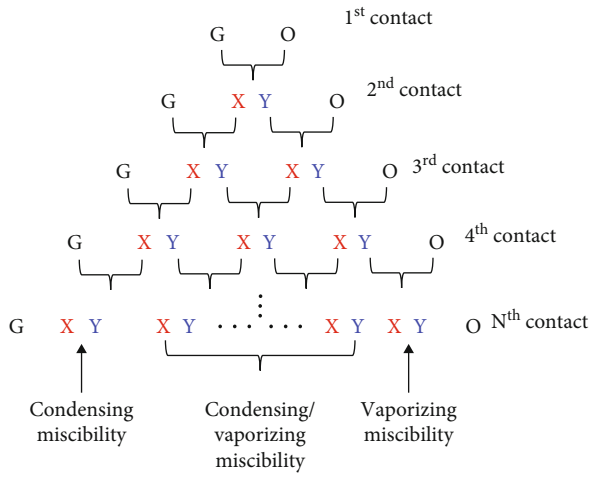


Figure 1: MMC model established by AHMADI [40].

or multiphase complex systems simply, quickly, and stably. The calculated results are in good agreement with the measured values of the slim tube experiment. It is suitable for the system with the combination of condensing and vaporizing drives, and it considers the influence of asphaltene precipitation and low-temperature conditions on MMP [42, 43]. Therefore, the predicted value of MMP by MMC is more accurate than other theoretical calculation methods. However, the MMC also has some problems. For example, it is incorrect to judge the initial value, and the solution is not only one.

In conclusion, the experimental method generally has a long period and a high cost, while the theoretical calculation method is relatively faster and more accurate. However, most of these two types of methods currently obtain the MMP under bulk conditions, and there are few solutions for the MMP of the oil and gas two phases at the nanoscale. Therefore, a new, efficient, and accurate method to determine the MMP is proposed. In this paper, based on the modified Peng-Robinson equation of state (PR-EOS), a flash calculation model is established which takes into account the influence of the confinement effect at the nanoscale. Then the flash calculation model is used to judge whether the oil-gas two phases have reached an equilibrium state so as to calculate the interfacial tension between the two phases. Afterward, we use the extrapolation method to obtain the MMP of the oil and gas system at the nanoscale. Finally, the reliability of the model is verified by comparing the MMP obtained by the MMC method with the MMP obtained in this paper. In addition, the effects of confinement effect, reservoir temperature, hydrocarbon type, and nanopore size on the MMP are emphatically studied.

## 2. Materials and Methods

*2.1. Modified PR-EOS.* The equation of state is a mixture of theory and experience, which is used to express the P-V-T phase behavior of the fluid. It can not only accurately predict the equilibrium state of oil and gas in two phases but also analyze and determine the changes in the two-phase conditions, especially the change in the critical point trend. Scholars have done a lot of researches on the equation of state, mainly including the Redlich-Kwong equation of state (RK-EOS), the Peng-Robinson equation of state (PR-EOS), and the modified PR-EOS [21, 44].

In this paper, the modified PR-EOS is used to establish the flash calculation model in nanopores [44]. And the modified PR-EOS is shown as follows:

$$P = \frac{RT}{v-b} - \frac{a}{v(v+b)+b(v-b)}, \tag{1}$$

where

$$\begin{aligned} a &= \frac{0.45724R^2T_c^2}{P_c}\alpha(T), \\ b &= \frac{0.0778RT_c}{P_c}, \\ \alpha(T) &= \left[1+m\left(1-\sqrt{T_r}\right)\right]^2, \\ m &= 0.37464 + 1.54226\omega - 0.26992\omega^2, \end{aligned} \tag{2}$$

where $P$ is the system pressure; $T$ is the system temperature; $R$ is the universal gas constant; $v$ is the molar volume; $a$ and $b$ are the gravitational coefficient and the repulsion coefficient separately; $T_c$ and $P_c$ are the critical temperature and the critical pressure in bulk phase separately; $T_r$ is the reduced temperature; $\omega$ is the acentric factor; $\alpha$ is the adjustable temperature function.

However, considering the large capillary pressure and confinement effect in nanopores, the critical temperature and the critical pressure of the fluid in nanopores are calculated according to the equations which are related to the Lennard-Jones diameter ($\sigma_{LJ}$) and the pore radius in this paper [45].

$$\begin{aligned} T_{cp} &= T_c - T_c\left[0.9409\frac{\sigma_{LJ}}{r_p} - 0.2415\left(\frac{\sigma_{LJ}}{r_p}\right)^2\right], \\ P_{cp} &= P_c - P_c\left[0.9409\frac{\sigma_{LJ}}{r_p} - 0.2415\left(\frac{\sigma_{LJ}}{r_p}\right)^2\right], \\ \sigma_{LJ} &= 0.244\sqrt[3]{\frac{T_c}{P_c}}, \end{aligned} \tag{3}$$

where $T_{cp}$ is the critical temperature in nanopores; $P_{cp}$ is the critical pressure in nanopores; $r_p$ is the nanopore radius.

*2.2. Calculation Derivation of MMP.* The flash calculation model based on the modified PR-EOS determines whether the oil and gas phases in the nanosystem reach an equilibrium state according to the equality of the fugacity of the two phases. After the oil-gas two phases are in equilibrium,

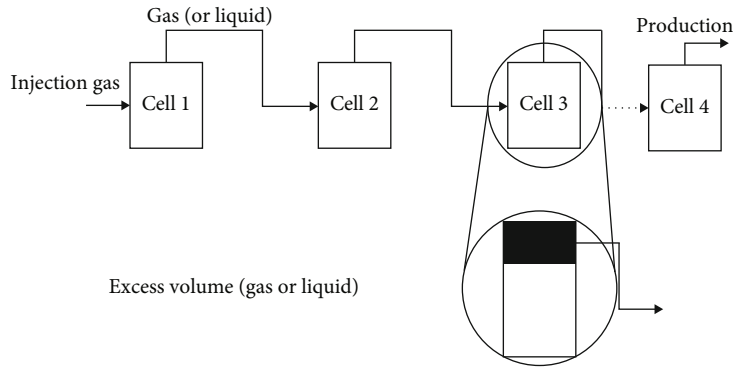


Figure 2: MMC model established by JAUBERT [41].

the interfacial tension between the two phases is calculated using the following formulas. When the extrapolated interfacial tension is zero, the corresponding pressure is the MMP of the $CO_2$-oil system in nanopores. At the same time, considering that the Newton iteration method is involved in many parts of the calculation process and artificial calculation is more complex and time-consuming, so in this paper, the MATLAB software to realize the calculation of the flash calculation model was used. The flow chart of the flash calculation model based on the modified PR-EOS for phase properties estimate the Macleod-Sugden equation for interfacial tension calculation, and the MMP calculation in nanopores is shown in Figure 3. In addition, the relevant calculation formulas and equations can be found in the supporting information.

According to the research requirement, we need to set the following parameters before the calculation: initial capillary pressure ($P_{cap}$) is 0 atm; oil and gas contact angle ($\theta$) is 30°; universal gas constant ($R$) is 82.06 atm·cm$^3$/(mol·K); calculation error is 0.0005.

## 3. Results and Discussion

*3.1. Model Validation.* In order to verify the reliability of the proposed model, the MMP of the $CO_2$-octane system is calculated and compared with the MMC model at 373 K and 5 nm pore radius. The relationships between IFTs and pressures are shown in Figure 4. The interfacial tension decreases with the increase of pressure, which shows a good linear relationship. The fitting result is as follows:

$$\mathrm{IFT} = -0.05813P + 5.53, \tag{4}$$

where $P$ is the pressure of the system and IFT is the interfacial tension of oil and gas phases. The MMP of the $CO_2$-octane system can be obtained by extrapolating to the corresponding pressure where the IFT is zero. According to the linear relationship, the MMP of this system can be predicted to be 9.64 Mpa. For the MMC model, the calculated MMP is around 9.7 MPa (as shown in Figure 5). The relative error between the calculated MMP in this research and the MMP calculated by the MMC model is 0.62%. It seems that our proposed model is feasible to predict the MMP at the nanoscale, which has high reliability and good prediction. Besides, the estimated IFT in this research is also compared with that of the experimental IFT data in reference [17], as shown in Figure 6. It is found that the simulated results are close to those of the reference [17], with an average absolute relative deviation (AARD) of about 7.2%.

*3.2. Confinement Effect on MMP at the Nanoscale.* The influence of the confinement effect on MMP at the nanoscale is shown in Figure 7. The MMPs of the $CO_2$-octane system increase with increasing temperature for both at the nanoscale and in the bulk phase. At the nanoscale, the MMP increases with temperature initially, and then the growth rate for MMP slowed down when the temperature is over 343.15 K. However, for the bulk phase, the MMP increases rapidly as the temperature increases. Besides, it shows that the MMP in nanopores is generally lower than that in the bulk phase. It seems that the influence of the confinement effect on MMP at the nanoscale cannot be ignored. When the temperature is low (shown in Figure 8), the MMP difference in the bulk phase and at the nanoscale is small, and the relative error is less than 10%. With the temperature rising, the difference between the MMP at the nanoscale and the MMP in the bulk phase is increasing. When the temperature is 372.53 K, the relative error reaches more than 30%. Therefore, it is speculated that the confinement effect has a stronger influence on MMP in the nanosystem at higher temperatures.

In the process of $CO_2$ injection displacement in a shale reservoir, the intermolecular interaction force at the nanoscale is strong and cannot be ignored. The adsorption layer is formed on the surface of nanopores, which have a great influence on the properties of fluid [46]. The physical properties of the fluid in nanopores are often different from the measured values in the laboratory. The influence of the confinement effect at the nanoscale can make the critical temperature, critical pressure, interfacial tension, and other properties of the fluid change greatly. It is generally believed that the bubble pressure and interfacial tension in nanopores are lower than those in the bulk phase. And the smaller the nanopore size, the more significant the difference with the bulk phase. Therefore, the MMP of $CO_2$ and crude oil at the nanoscale is different from

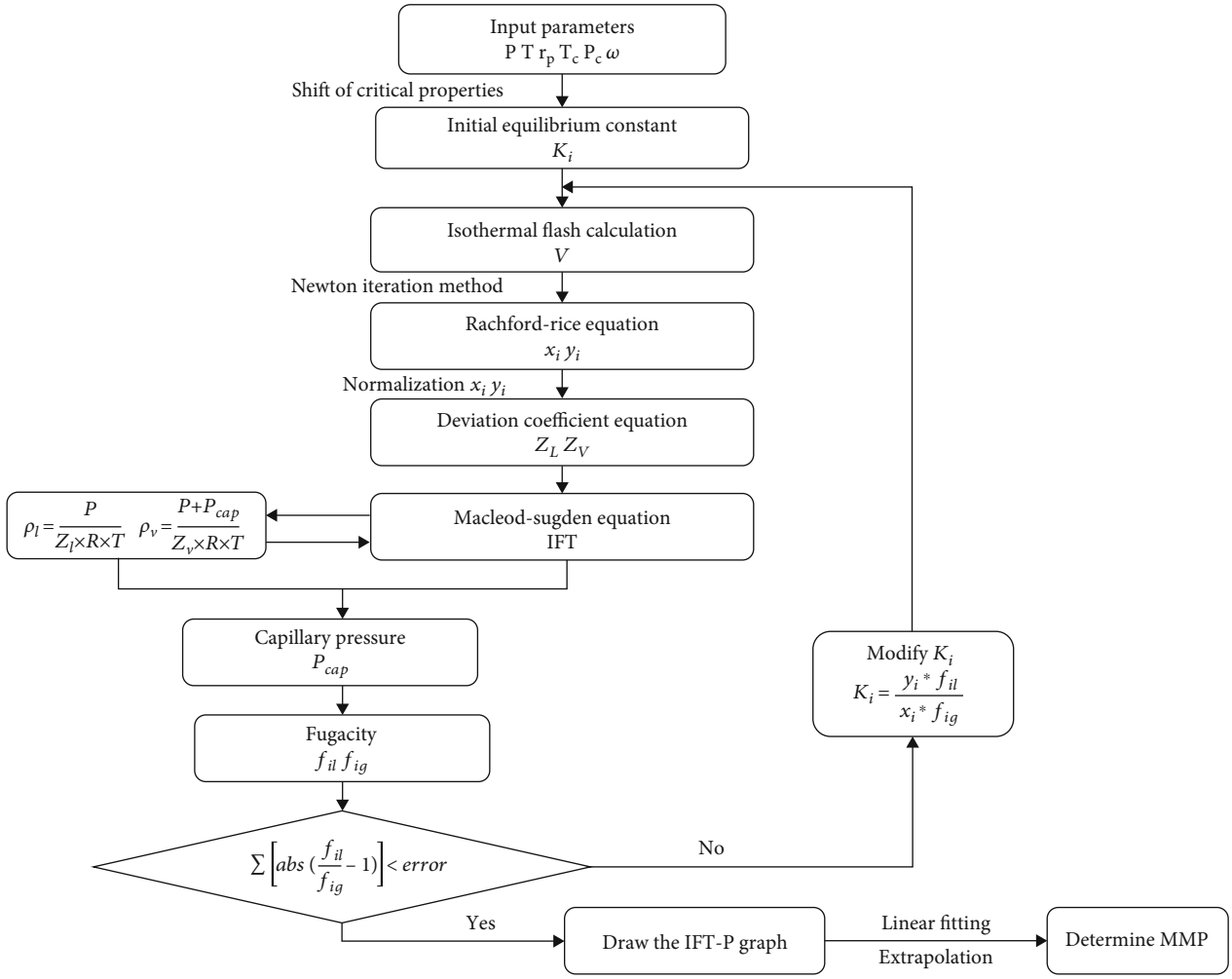


Figure 3: Flow chart for MMP calculation.

that in the bulk phase due to the confinement effect in nanopores. The measured MMP at the nanoscale is generally smaller than that in the bulk phase.

*3.3. Effect of Temperature on MMP.* The effect of temperature on MMPs for $CO_2$ and different alkane systems is shown in Figure 9. The simulation results show that the MMP increases with the rising temperature. For all of the alkane systems, the MMP increases first, and then the increasing rate slows down. This phenomenon is particularly obvious in $CO_2$-butane and $CO_2$-hexane systems. For $CO_2$-octane and $CO_2$-decane systems, the MMP is more sensitive to the higher temperature compared to the alkane with a lower carbon atom number.

The influences of reservoir temperature on MMP are mainly reflected in the changes in the P-V-T properties of crude oil, such as the density, viscosity, and dissolved gas-oil ratio. Most scholars have found that the MMP increases when the temperature rises [21, 23]. The MMP is in proportion to the reservoir temperature. The density of $CO_2$ becomes smaller with the continuous increase in temperature when other conditions in the reservoir remain the same, which results in the weak solubility of $CO_2$, and less $CO_2$ is dissolved in crude oil. At high temperature, the $CO_2$ extraction amount of the light hydrocarbon components decreases, which can also lead to an increase in MMP. Liu et al. explained the effect of reservoir temperature and pressure on the oil-gas interfacial tension at the microlevel [47]. The reservoir temperature and pressure affect the two-phase interfacial tension by changing $CO_2$ density and oil-gas thermodynamic parameters, which ulteriorly affect the MMP.

*3.4. Effect of Hydrocarbon Type on MMP.* The effects of hydrocarbon type on MMP at different temperatures are shown in Figure 10. As the carbon atom number in alkanes increases, the MMP gets enhanced. Therefore, crude oil which has more light hydrocarbon components is easier to reach the miscible state in actual oil fields. In addition, it is found that the relationship between MMP and the number of carbon atoms is close to a straight line. Through linear fitting, it is found that the fitting degrees at different temperatures are different, but they are all close to 1. So, it is inferred that MMP has a linear relationship with the number of carbon atoms in n-alkanes.

Due to the diversity of the crude oil components and properties, the displacement mechanism of $CO_2$ and crude

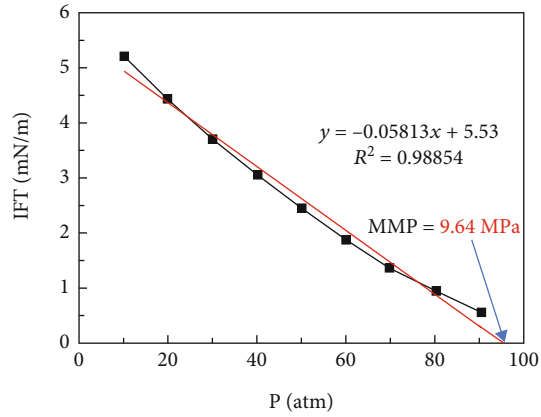


Figure 4: The relationships between IFTs and pressures for the $CO_2$-octane system.

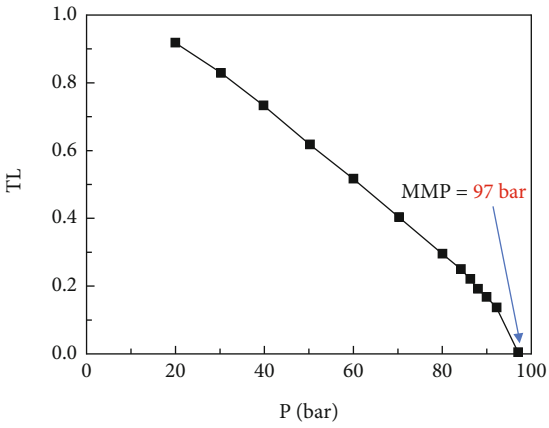


Figure 5: The calculated MMP by the MMC model.

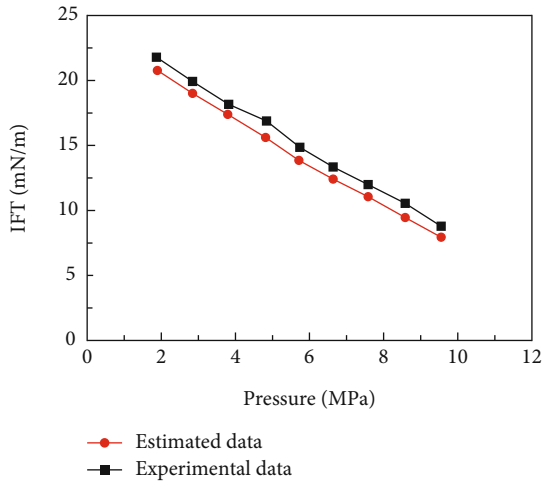


Figure 6: Comparison between calculated vapor–liquid IFTs and experimental. Data [1] for $CO_2$/n-$C_{16}H_{34}$ at 79.6°C.

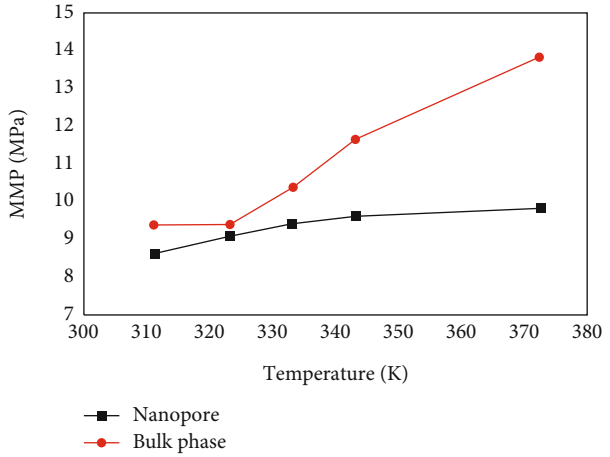


Figure 7: The calculated MMPs of the $CO_2$-octane system at the pore radius of 5 nm and the experimental MMPs in the bulk phase at $T$ = 311.15 K to 372.53 K.

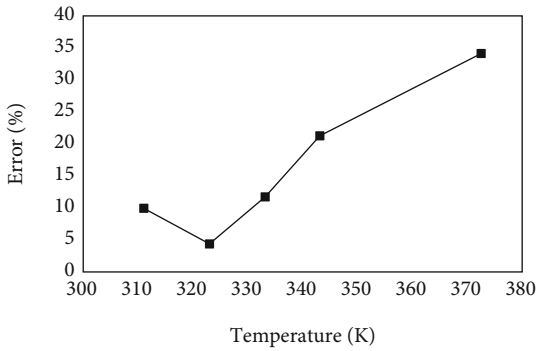


Figure 8: The relative errors between the calculated MMPs of the $CO_2$-octane system at the pore radius of 5 nm and the experimental MMPs in the bulk phase at $T$ = 311.15 K to 372.53 K.

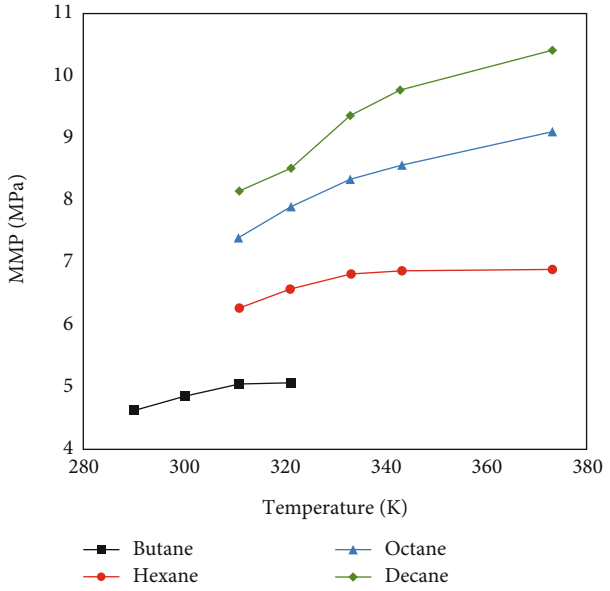


Figure 9: The effect of temperature on MMP of $CO_2$ and pure alkane system ($C_4H_{10}$, $C_6H_{14}$, $C_8H_{18}$, and $C_{10}H_{22}$) at $T$ = 290.15 K to 373.15 K with 5 nm pore radius.

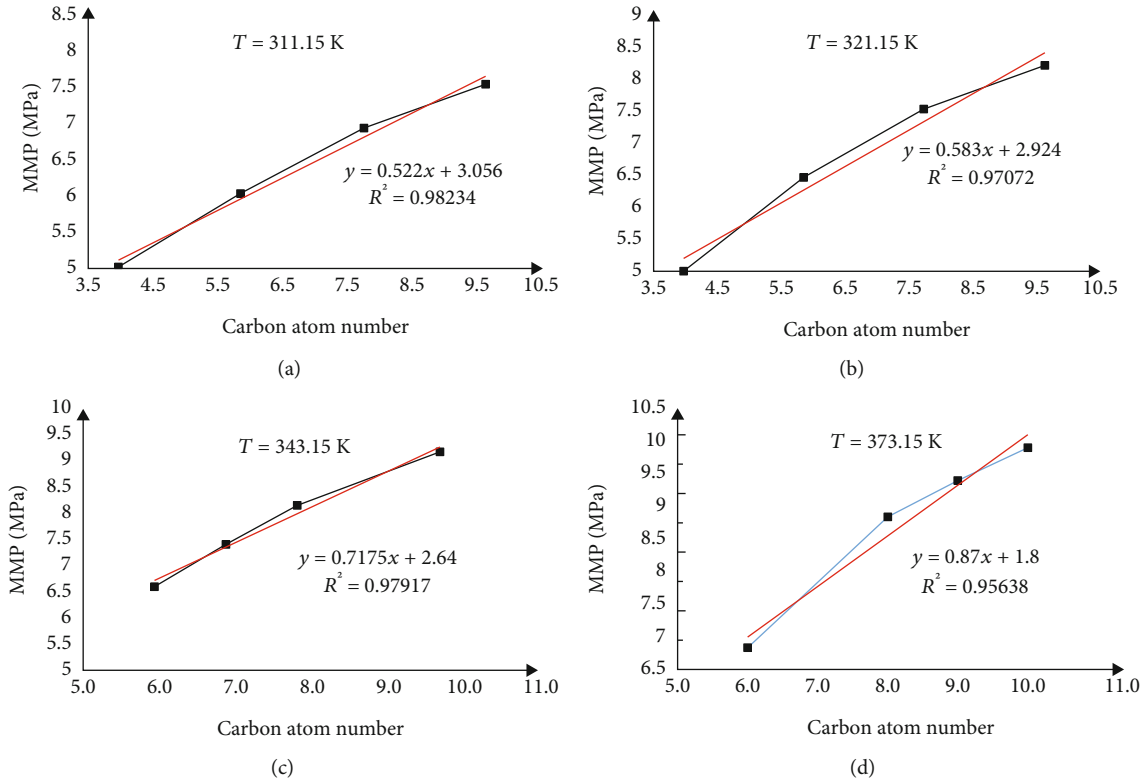


Figure 10: The relationship between MMPs and carbon atom number ($C_4H_{10}$, $C_6H_{14}$, $C_8H_{18}$, and $C_{10}H_{22}$) at 5 nm pore radius: (a) 311.15 K; (b) 321.15 K; (c) 343.15 K; (d) 373.15 K.

oil is also different. Crude oil is usually divided into three representative pseudo-components according to the number of carbon atoms: volatile light components ($CH_4$ and $N_2$), intermediate components ($C_2$-$C_4$ or $C_2$-$C_6$), and heavy components ($C_{5+}$ or $C_{7+}$). Liu et al. found that the interfacial tension is positively correlated with the number of carbon atoms in the $CO_2$ and single-component oil phase system through the interfacial tension experiment [47]. The larger the carbon atom number, the greater the interfacial tension and the larger the MMP. In actual oil reservoirs, the variation of MMP is mainly related to the content of $C_2$-$C_6$ in crude oil. The MMP increased with the decrease of $C_2$-$C_6$ content, while it is positively correlated with the content of heavy components [48, 49]. This is mainly determined by the relationship between $CO_2$ extraction and the miscibility principle. During the contact between $CO_2$ and crude oil, the light components in the crude oil are continuously extracted and enriched in the $CO_2$ phase. After reaching a certain level, the miscibility of $CO_2$ and crude oil is realized. As the light components in the remaining oil continue to decrease, the pressure required for miscibility will also increase, which makes it difficult for $CO_2$ to be miscible with the remaining oil. Tang et al. also found that the more molar components of $C_2$-$C_6$ in crude oil components, the lower the MMP. Therefore, reservoirs with high light component content should be selected for $CO_2$ injection flooding, where $CO_2$ and crude oil can be miscible at low formation pressure. During $CO_2$ flooding, the adjustment of the injection-production scheme in time is the key to improving the oil recovery by monitoring and analyzing the miscible state in the reservoir. The bottom-hole flow pressure and injection pressure should be appropriately increased if the MMP of $CO_2$ and crude oil increases. Therefore, it is necessary to dynamically calculate and analyze the MMP of the reservoir to clarify the miscible conditions in the reservoir.

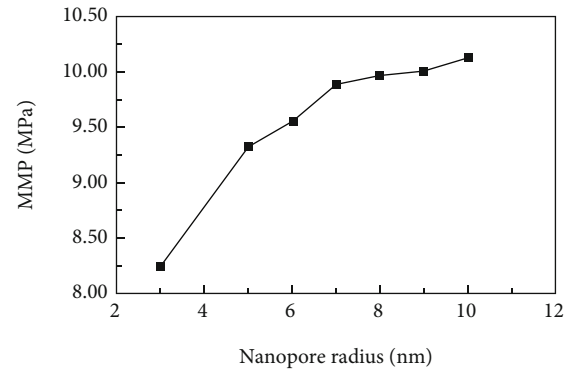


Figure 11: The MMPs of the $CO_2$-$C_{10}H_{22}$ system at $T = 344.15$ K with different nanopore radii (3, 5, 6, 7, 8, 9, and 10 nm).

*3.5. Effect of Nanopore Size on MMP.* The relationship between MMP and nanopore size is shown in Figure 11. It shows that the MMP has a positive correlation with the nanopore radius. At small nanopore size, the MMP increases rapidly with the rising nanopore radius. The MMP reduction in small nanopores is caused primarily by the critical point shift due to the confinement effect [46]. The

interactions between molecules and nanopore walls are decreased with increasing nanopore size, which significantly affects the interface between vapor and liquid phases and interfacial free energy. This results in a rapid increase in IFT and a rapid decrease in MMP at small nanopores.

However, the increasing trend of MMP begins to slow down gradually when the pore radius grows to a certain value. It can be inferred that when the nanopore radius is getting larger, the MMP of the $CO_2$-oil system in nanopores should be closer to the MMP in the bulk phase. Sun and Li found that MMP remains constant and is not affected by the confinement effect when the pore size is greater than 10 nm [46]. It is inferred that molecule-level phenomena no longer play an important role in affecting the phase behavior of $CO_2$ and crude oil within the nanopores (such as adsorption and nonhomogeneous density distributions in the nanopore). The distribution of the pore radius is the key factor when calculating the MMP in nanopores. It indicates that the average pore radius cannot be directly used to calculate MMP as the MMP (especially for larger pore radius) is no longer linear with the pore radius. At large nanopore size, Bao et al. also found that the MMP of the $CO_2$-decane system has almost no significant difference from the MMP by using micro-nanofluidic technology [50]. With the rising nanopore size, the MMP at the nanoscale and the MMP in the bulk phase are getting closer.

## 4. Conclusions

All major conclusions from this work are shown in the following section:

(1) An MMP calculation method is proposed through the extrapolation of IFT for the $CO_2$-oil system based on modified PR-EOS at the nanoscale. The relative error between the calculated MMP in this research and the MMC method is 0.62% at 373 K and a 5 nm pore radius. It indicates that the proposed method is efficient to predict the MMP accurately with less calculation

(2) The calculated MMP at the nanoscale is generally smaller than that in the bulk phase. At the same time, the confinement effect has a stronger influence on the MMP in the nanopores at a higher temperature

(3) At the same reservoir temperature, MMP is positively correlated with the carbon atom number of n-alkanes. Therefore, crude oil which has more light hydrocarbon components is easier to reach the miscible state

(4) The MMP has a positive correlation with the nanopore radius. When the nanopore radius is getting larger, the MMP of the $CO_2$-oil system in nanopores would be closer to the MMP in the bulk phase. In addition, the average pore radius cannot be directly used to calculate MMP as the MMP (especially for larger pore radius) is no longer linear with the pore radius

## Data Availability

The data used to support the findings of the work are available from the corresponding author upon request.

## Conflicts of Interest

The submission has been received explicitly from all co-authors. And authors whose names appear on the submission have contributed sufficiently to the scientific work and therefore share collective responsibility and accountability for the results.

## Acknowledgments

This research was funded by the Sinopec scientific and technological research project "Research on optimization design of pressure drive development technology for increasing speed and efficiency" (grant number P21072-2) and "Research on flow field characterization and development optimization control technology of high water cut old oil fields" (grant number P21017).

## References

[1] D. Fan, Z. Wang, W. Li, and Y. Wang, "Analysis and prospects of oil and gas resource situation at home and abroad in 2021," *China Mining Magazine*, vol. 31, no. 1, pp. 26–31, 2022.

[2] W. Zhao, S. Hu, L. Hou et al., "Types and resource potential of continental shale oil in China and its boundary with tight oil," *Petroleum Exploration and Development*, vol. 47, no. 1, pp. 1–11, 2020.

[3] L. Zhou, Z. Han, D. Zhang, J. Ren, Z. Feng, and C. Zhang, "Characteristics of incremental proven oil and natural gas geological reserves in China," *Xinjiang Petroleum Geology*, vol. 43, no. 1, pp. 115–121, 2022.

[4] J. Du, S. Hu, Z. Pang, S. Lin, L. Hou, and R. Zhu, "The types, potentials and prospects of continental shale oil in China," *China Petroleum Exploration*, vol. 24, no. 5, pp. 560–568, 2019.

[5] W. Yang, J. Li, J. Zhao, and Z. Huang, "Qualitative and quantitative study of micro-pore structures of Longmaxi formation shale in Fuling area," *Sichuan Basin. Petroleum Geology & Experiment*, vol. 40, no. 1, pp. 97–102, 2018.

[6] H. Song, *Feasibility Study on Effective Development Mode of Shale Oil Reservoir*, China University of Petroleum (Beijing), 2017.

[7] Y. Liu and Z. Rui, "A storage-driven $CO_2$ EOR for a net-zero emission target," *Engineering*, vol. 18, pp. 79–87, 2022.

[8] Y. Liu, Z. Rui, T. Yang, and B. Dindoruk, "Using propanol as an additive to $CO_2$ for improving $CO_2$ utilization and storage in oil reservoirs," *Applied Energy*, vol. 311, article 118640, 2022.

[9] Y. Liu, X. Ma, H. Li, and J. Hou, "Competitive adsorption behavior of hydrocarbon(s)/$CO_2$ mixtures in a double-nanopore system using molecular simulations," *Fuel*, vol. 252, pp. 612–621, 2019.

[10] Y. Zhang, J. Sheng, Q. Li, P. Song, Y. Chen, and J. Qin, "Advances in the application of $CO_2$ stimulation technology," *Special Oil & Gas Reservoirs*, vol. 28, no. 6, pp. 1–10, 2021.

[11] C. Huang, L. Huo, and C. Wu, "Progress and prospect of $CO_2$ resource utilization technology based on unconventional oil and gas development," *Unconventional Oil & Gas*, vol. 9, no. 1, pp. 1–9, 2022.

[12] G. Li, Z. Lei, W. Dong, H. Wang, X. Zheng, and J. Tan, "Progress, challenges and prospects of unconventional oil and gas development of CNPC," *China Petroleum Exploration*, vol. 27, no. 1, pp. 1–11, 2022.

[13] C. Wang, *Experimental Study on $CO_2$ Injection in Tight Reservoirs*, Southwest Petroleum University, 2016.

[14] L. Fan and B. Li, "Present research situation and Prospect of $CO_2$ injection for enhanced oil recovery in shale reservoir," *Petrochemical Industry Application*, vol. 41, no. 2, pp. 1–7, 2022.

[15] Y. Yang, L. Lei, and J. Sheng, "Further discuss the roles of soaking time and pressure depletion rate in gas huff-n-puff process in fractured liquid-rich shale reservoirs," in *Paper Presented at the SPE Annual Technical Conference and Exhibition*, Dubai, UAE, 2016.

[16] W. Zhang, J. Xu, R. Jiang et al., "Employing a quad-porosity numerical model to analyze the productivity of shale gas reservoir," *Journal of Petroleum Science and Engineering*, vol. 157, pp. 1046–1055, 2017.

[17] X. Cui, L. Zheng, Z. Liu, P. Cui, and D. Du, "Determination of the minimum miscibility pressure of the $CO_2$/oil system based on quantification of the oil droplet volume reduction behavior," *Colloids and Surfaces A: Physicochemical and Engineering Aspects*, vol. 653, article 130058, 2022.

[18] X. Wang, X. Cui, F. Wang et al., "Miscibility characteristics of the $CO_2$/n-hexadecane system with presence of water component based on the phase equilibrium calculation on the interface region," *Colloids and Surfaces A: Physicochemical and Engineering Aspects*, vol. 629, article 127463, 2021.

[19] F. M. Orr Jr. and K. Jessen, "An analysis of the vanishing interfacial tension technique for determination of minimum miscibility pressure," *Fluid Phase Equilibria*, vol. 255, no. 2, pp. 99–109, 2007.

[20] K. Jessen and F. M. Orr, "On interfacial-tension measurements to estimate minimum miscibility pressures," *SPE Reservoir Evaluation & Engineering*, vol. 11, no. 5, pp. 933–939, 2008.

[21] K. Zhang, N. Jia, S. Li, and L. Liu, "Millimeter to nanometer-scale tight oil-$CO_2$ solubility parameter and minimum miscibility pressure calculations," *Fuel*, vol. 220, pp. 645–653, 2018.

[22] F. Yang and P. Yu, "Technical standard of minimum miscible flooding pressure determination with slim tube experiment," *Special Oil and Gas Reservoirs*, vol. 26, no. 6, pp. 118–122, 2019.

[23] F. Qian, *Study on the Influence of Formation Oil between $CO_2$ and Minimum Miscibility Pressure*, Northeast Petroleum University, 2020.

[24] R. Sun, S. Lei, D. Liu, T. Xu, C. Liu, and S. Wang, "Experimental studies on flow pattern transition temperature of heavy oils," in *Paper Presented at the International Conference on New Energy and Renewable Resources*, Guangzhou, China, 2015.

[25] M. Liang, H. Yuan, Y. Yang, Y. Yang, and J. Lin, "Research progress on miscible gas displacement and determination of minimum miscibility pressure," *Journal of Southwest Petroleum University (Science & Technology Edition)*, vol. 39, no. 5, pp. 101–112, 2017.

[26] Q. Ma, S. Yang, M. Wang, J. Chen, and M. Wang, "Experimental investigation on minimum miscible pressure of the tight oil reservoir in Jimsar Sag," *Xinjiang. Journal of Liaoning Shihua University*, vol. 40, no. 1, pp. 35–38, 2020.

[27] Y. Ding, *A New Method for Testing the Miscibility Pressure of $CO_2$ Miscible Flooding*, Southwest Petroleum University, 2018.

[28] H. Shojaei, R. Rastegar, and J. Kristian, "Experimental and modeling study of multicontact miscible displacements," in *Paper presented at the SPE Improved Oil Recovery Symposium*, Tulsa, Oklahoma, USA, April 2012.

[29] F. Yang and P. Yu, "Progress of research on determination of minimum miscibility pressure for gas injection miscible flooding," *Advances in Fine Petrochemicals*, vol. 21, no. 3, pp. 1–11, 2020.

[30] M. Nobakht, S. Moghadam, and Y. Gu, "Determination of $CO_2$ minimum miscibility pressure from measured and predicted equilibrium interfacial tensions," *Industrial and Engineering Chemistry Research*, vol. 47, no. 22, pp. 8918–8925, 2008.

[31] G. Zhang, J. Liu, X. Zhang, J. Xu, P. Gao, and Y. Zu, "Study on determine methods of minimum miscibility pressure of hydrocarbon injection miscible flooding," *Drilling and Production Technology*, vol. 31, no. 3, pp. 99–102, 2008.

[32] Y. Liu, *Evaluation of Huaqing Oilfield C6 $CO_2$ Flooding Foam System*, Xi'an Shiyou University, 2012.

[33] H. Zhou, *Experimental Investigation on $CO_2$ Miscible Drive in Ultra-Low Permeability Reservoirs*, Daqing Petroleum Institute, 2008.

[34] K. Zhang, N. Jia, S. Li, and L. Liu, "Nanoscale-extended correlation to calculate gas solvent minimum miscibility pressures in tight oil reservoirs," *Journal of Petroleum Science and Engineering*, vol. 171, pp. 1455–1465, 2018.

[35] A. Hemmati-Sarapardeh, E. Mohagheghian, M. Fathinasab, and A. H. Mohammadi, "Determination of minimum miscibility pressure in $N_2$-crude oil system: a robust compositional model," *Fuel*, vol. 182, pp. 402–410, 2016.

[36] A. Barati-Harooni, A. Najafi-Marghmaleki, S. A. Hoseinpour et al., "Estimation of minimum miscibility pressure (MMP) in enhanced oil recovery (EOR) process by $N_2$ flooding using different computational schemes," *Fuel*, vol. 235, pp. 1455–1474, 2019.

[37] X. Zheng, Y. Lei, W. Ding, and Y. Yang, "Research on prediction method of the minimum miscible pressure for carbon dioxide flooding in low permeability reservoirs," *Contemporary Chemical Industry*, vol. 50, no. 11, pp. 2636–2643, 2021.

[38] F. Yang, P. Yu, and X. Zhang, "Multiple-mixing-cell model for calculation of minimum miscibility pressure controlled by tie-line length," *Geofluids*, vol. 2020, Article ID 9587254, 8 pages, 2020.

[39] K. Ahmadi and R. T. Johns, "Multiple-mixing-cell method for MMP calculations," *SPE Journal*, vol. 16, no. 4, pp. 733–742, 2011.

[40] J. N. Jaubert, L. Wolff, E. Neau, and L. Avaullee, "A very simple multiple mixing cell calculation to compute the minimum miscibility pressure whatever the displacement mechanism," *Industrial and Engineering Chemistry Research*, vol. 37, no. 12, pp. 4854–4859, 1998.

[41] R. Li and H. Li, "A modified multiple-mixing-cell algorithm for minimum miscibility pressure prediction with the consideration of the asphaltene-precipitation effect," *Industrial and Engineering Chemistry Research*, vol. 58, no. 33, pp. 15332–15343, 2019.

[42] L. Li, S. Khorsandi, R. T. Johns, and K. Ahmadi, "Multiple-mixing-cell method for three-hydrocarbon-phase displacements," *SPE Journal*, vol. 20, no. 6, pp. 1339–1349, 2015.

[43] D. Peng and D. Robinson, "A new two-constant equation of state," *Industrial & Engineering Chemistry Research*, vol. 15, no. 1, pp. 59–64, 1976.

[44] G. J. Zarragoicoechea and V. A. Kuz, "Critical shift of a confined fluid in a nanopore," *Fluid Phase Equilibria*, vol. 220, no. 1, pp. 7–9, 2004.

[45] L. Wang, E. Parsa, Y. Gao et al., "Experimental study and modeling of the effect of nanoconfinement on hydrocarbon phase behavior in unconventional reservoirs," in *Paper Presented at the SPE Western North American and Rocky Mountain Joint Meetng*, Denver, Colorado, April 2014.

[46] H. Sun and H. Li, "Minimum miscibility pressure determination in confined nanopores considering pore size distribution of tight/shale formations," *Fuel*, vol. 286, no. 2, article 119450, 2021.

[47] X. Liu, M. Mutailipu, J. Zhao, and Y. Liu, "Comparative analysis of four neural network models on the estimation of $CO_2$–brine interfacial tension," *ACS Omega*, vol. 6, no. 6, pp. 4282–4288, 2021.

[48] Y. Tang, X. Zhao, and Y. Wang, "Analysis of influence factor of minimum miscible pressure of $CO_2$," *Reservoir Evaluation and Development*, vol. 8, no. 4, pp. 42–45, 2018.

[49] B. Han, Z. Zhai, W. Yu et al., "Dynamic analysis of minimum miscibility pressure during $CO_2$ flooding reservoirs and its influencing factors," *Unconventional Oil & Gas*, vol. 9, no. 1, pp. 98–104, 2022.

[50] B. Bao, J. Feng, J. Qiu, and S. Zhao, "Direct measurement of minimum miscibility pressure of Decane and $CO_2$ in nanoconfined channels," *ACS Omega*, vol. 6, no. 1, pp. 943–953, 2021.